

# Photoproduction of top quarks in coherent hadron-hadron interactions

V. P. Gonçalves

*Instituto de Física e Matemática, Universidade Federal de Pelotas,  
Caixa Postal 354, CEP 96010-900 Pelotas, Rio Grande do Sul, Brazil*  
(Received 26 August 2013; published 25 September 2013)

In this paper we study the photoproduction of top quarks in coherent  $pp$ ,  $pPb$ , and  $PbPb$  interactions at LHC energies in the collinear formalism. We present our predictions for the total cross sections, event rates, and rapidity distributions. The dependence in the parton distributions used in the calculations is analyzed, and the effect of the shadowing corrections is estimated.

DOI: [10.1103/PhysRevD.88.054025](https://doi.org/10.1103/PhysRevD.88.054025)

PACS numbers: 12.38.-t, 13.60.Hb

Heavy quark production in hard collisions has been considered as a clean test of perturbative quantum chromodynamics (QCD) (For a review see, e.g., Ref [1]). This process provides not only many tests of perturbative QCD but also some of the most important backgrounds to new physics processes, which have motivated an extensive phenomenology at DESY-HERA, Tevatron, and the LHC. These studies are mainly motivated by the strong dependence of the cross section on the behavior of the gluon distribution, which determines the QCD dynamics at high energies. In particular, the charm and bottom photoproduction on nucleon and nuclei targets has been studied in detail in, e.g., Ref. [2], considering the several available scenarios for the QCD dynamics at high energies. The results of those analyses show that future electron-proton (nucleus) colliders [3,4] probably could determine the behavior of the gluon distribution at small values of the Bjorken- $x$  variable. Along these lines, in Refs. [5] we have analyzed the possibility of using the LHC as a photon-hadron collider and studied the bottom and charm production assuming distinct formalisms for the QCD evolution (for more recent studies, see [6]). The basic idea is that at large impact parameter ( $b > R_{h_1} + R_{h_2}$ , where  $R_h$  is the hadron radius) and ultrarelativistic energies, the electromagnetic interaction is expected to dominate. In heavy ion collisions, the heavy nuclei give rise to strong electromagnetic fields due to the coherent action of all protons in the nucleus, which can interact with each other. Similarly, this also occurs when considering ultrarelativistic protons in  $pp$  collisions. The photon emitted from the electromagnetic field of one of the two colliding hadrons can interact with one photon of the other hadron (two-photon process) or directly with the other hadron (photon-hadron process). In particular, in photon-hadron interactions, the total cross section for a given process can be factorized in terms of the equivalent flux of photons into the hadron projectile and the photon-target production cross section. The main advantage of using colliding hadrons and nuclear beams for studying photon-induced interactions is the high equivalent photon energies and luminosities that can be achieved at existing and future accelerators (for a review see Ref. [7]). Consequently, studies of  $\gamma p(A)$  interactions at the LHC

could provide valuable information on the heavy quark production at high energies. Recent experimental results from CDF [8] at Tevatron, STAR [9] and PHENIX [10] at RHIC, and ALICE [11] and LHCb [12] at the LHC have demonstrated that the study of coherent interactions in these colliders is feasible and that the data can be used to constrain the description of the hadronic structure at high energies.

In this paper we extend the previous analysis on heavy quark photoproduction for the case of the top quark, which plays a special role in the standard model, in particular in the electroweak symmetry breaking. Precise measurements of its properties and interactions may also reveal effects from new physics (For a recent review, see Ref. [13]). Although several properties of the top quark have been examined in the last eighteen years at the Tevatron, the collected statistics were small. In contrast, they are expected to be largely produced at the LHC. Our goal is to verify if the photoproduction of top quarks in coherent interactions at the LHC could also be used to improve our knowledge of its properties (For previous studies see Refs. [7,14]). It is important to emphasize that the photoproduction of top quarks was not studied in the HERA  $ep$  collider, and its experimental analysis still is an open question, which also motivates the study of the production of top quarks in coherent interactions.

The photoproduction of top quarks in a coherent hadron-hadron collision is represented in Fig. 1 and its cross section is given by

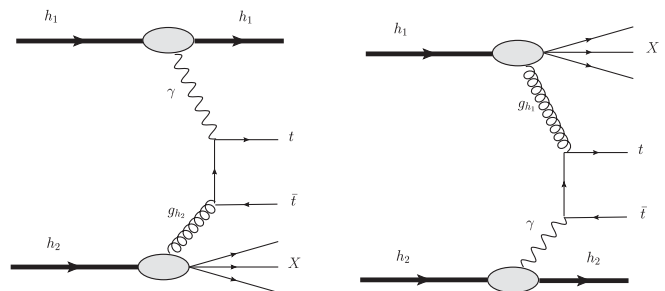


FIG. 1. The mechanism for the photoproduction of top quarks in coherent hadron-hadron interactions.

$$\begin{aligned}
& \sigma(h_1 + h_2 \rightarrow h \otimes \bar{t} + X) \\
&= \int d\omega \frac{dN}{d\omega} \Big|_{h_1} \sigma_{\gamma h_2 \rightarrow \bar{t}X}(W_{\gamma h_2}) \\
&+ \int d\omega \frac{dN}{d\omega} \Big|_{h_2} \sigma_{\gamma h_1 \rightarrow \bar{t}X}(W_{\gamma h_1}), \quad (1)
\end{aligned}$$

where  $\otimes$  represents the presence of one rapidity gap in the final state,  $\omega$  is the photon energy in the center-of-mass frame (c.m.s.),  $\frac{dN}{d\omega} \Big|_{h_i}$  is the equivalent photon flux for the hadron  $h_i$ , and  $W_{\gamma h}$  is the c.m.s. photon-hadron energy given by  $W_{\gamma h}^2 = 2\omega\sqrt{s}$ , where  $\sqrt{s}$  is the c.m.s. energy of the hadron-hadron system. Considering the requirement that photoproduction is not accompanied by hadronic interaction (ultraperipheral collision) an analytic approximation for the equivalent photon flux of a nuclei can be calculated, which is given by [7]

$$\frac{dN}{d\omega} \Big|_A = \frac{2Z^2\alpha_{em}}{\pi\omega} \left[ \bar{\eta}K_0(\bar{\eta})K_1(\bar{\eta}) - \frac{\bar{\eta}^2}{2} \mathcal{U}(\bar{\eta}) \right], \quad (2)$$

where  $K_0(\eta)$  and  $K_1(\eta)$  are the modified Bessel functions,  $\bar{\eta} = \omega(R_{h_1} + R_{h_2})/\gamma_L$  and  $\mathcal{U}(\bar{\eta}) = K_1^2(\bar{\eta}) - K_0^2(\bar{\eta})$ . Moreover,  $\gamma_L$  is the Lorentz boost of a single beam, and we consider  $R_p = 0.6$  fm and  $R_A = 1.2A^{1/3}$  fm in our calculations for  $pPb$  and  $PbPb$  collisions. It is important to emphasize that Eq. (2) was calculated assuming that absorptive corrections can be disregarded at  $b > R_{h_1} + R_{h_2}$ , while at smaller  $b < R_{h_1} + R_{h_2}$  the photon flux is zero. A better estimate of the total flux obtained by taking the average over the target surface was proposed in Ref. [15]. Recent studies [6] indicate that the difference between the analytical approximation given by Eq. (2) and that proposed in Ref. [15] is of the order of 10% to 15%. For proton-proton interactions, we assume that the photon spectrum is given by [16]

$$\begin{aligned}
\frac{dN}{d\omega} \Big|_p &= \frac{\alpha_{em}}{2\pi\omega} \left[ 1 + \left( 1 - \frac{2\omega}{\sqrt{s}} \right)^2 \right] \\
&\times \left( \ln \Omega - \frac{11}{6} + \frac{3}{\Omega} - \frac{3}{2\Omega^2} + \frac{1}{3\Omega^3} \right), \quad (3)
\end{aligned}$$

with the notation  $\Omega = 1 + [(0.71 \text{ GeV}^2)/Q_{\min}^2]$  and  $Q_{\min}^2 = \omega^2/[\gamma_L^2(1 - 2\omega/\sqrt{s})] \approx (\omega/\gamma_L)^2$ . This expression is derived considering the Weizsäcker-Williams method of virtual photons and using an elastic proton form factor (for more details see Refs. [16,17]). Equation (1) takes into account the fact that the incoming hadrons can act as both target and photon emitter. The experimental separation for such events is, in principle, relatively easy. As photon emission is coherent over the hadron and the photon is colorless, we expect the events to be characterized by an intact recoiled hadron (tagged hadron) and a one-rapidity gap pattern (for a detailed discussion, see [7]).

The photon-proton cross section can be calculated considering different theoretical scenarios [18]. In this paper we consider the collinear factorization approach, where the cross sections involving incoming hadrons are given, at all orders, by the convolution of intrinsically nonperturbative, but universal, quantities—the parton densities, with perturbatively calculable hard matrix elements, which are process dependent. In this approach, all partons involved are assumed to be on mass shell, carrying only longitudinal momenta, and their transverse momenta are neglected in the QCD matrix elements. In particular, the cross section for the photoproduction of heavy quarks is given in terms of the convolution between the elementary cross section for the subprocess  $\gamma g \rightarrow Q\bar{Q}$  and the probability of finding a gluon inside the hadron, namely the gluon distribution. At leading order, the top quark photoproduction cross section is given by [19]

$$\begin{aligned}
& \sigma_{\gamma h \rightarrow \bar{t}X}(W_{\gamma h}) \\
&= 4\pi e_t^2 \int_{4m_t^2}^{W_{\gamma h}^2} \frac{dM_{\bar{t}t}^2}{M_{\bar{t}t}^4} \alpha_{em} \alpha_s(\mu_F^2) x g_h(x, \mu_F^2) \\
&\times \left[ \left( 1 + \beta - \frac{1}{2}\beta^2 \right) \ln \left( \frac{1 + \sqrt{1-\beta}}{1 - \sqrt{1-\beta}} \right) \right. \\
&\left. - (1 + \beta)\sqrt{1-\beta} \right], \quad (4)
\end{aligned}$$

where  $M_{\bar{t}t}$  is the invariant mass of the top quark pair, with  $x = M_{\bar{t}t}^2/W_{\gamma h}^2$ , and  $g_h(x, \mu_F^2)$  is the gluon density inside the hadron at the factorization scale  $\mu_F^2$ . In addition,  $m_t$  is the top quark mass,  $e_t$  is its electric charge, and  $\beta \equiv 4m_t^2/M_{\bar{t}t}^2$ . In our calculations we will use  $\mu_F^2 = 4m_t^2$ , with  $m_t = 173.0$  GeV. It should be noted that different choices for the factorization scale and quark mass produce distinct overall normalization to the total cross section at photon-nucleon interactions and that NLO corrections, which are small in comparison to the hadroproduction case, can be absorbed in these redefinitions of  $\mu_F^2$  and  $m_t^2$  [20]. In what follows, we will consider different parametrizations for the parton distributions. In particular, we use the MRST [21] and CT10 [22] parton distributions for the proton. In the nuclear case, we take into account the nuclear shadowing effects as given by the EPS09 parametrization [23], which is based on a global fit of the current nuclear data. Before we present our results, it is important to emphasize the typical values of  $x$ , which will be probed in coherent  $pp/pPb/PbPb$  collisions. Considering that for  $pp/pPb/PbPb$  collisions at LHC, the Lorentz factor is  $\gamma_L = 7455/4690/2930$  [7], we obtain that the maximum c.m.s.  $\gamma h$  energy will be  $W_{\gamma h} \approx 8390/1500/950$  GeV. Consequently, we obtain that for the top quark photoproduction in coherent interactions, we will probe the gluon distribution at  $x \geq 1.7 \times 10^{-3}$  in  $pp$  collisions,  $x \geq 5.3 \times 10^{-2}$  in  $pPb$  collisions, and  $x \geq 0.13$  in  $PbPb$  collisions.

Let us calculate the rapidity distribution and total cross section for the top quark photoproduction in coherent  $pp$ ,  $pPb$ , and  $PbPb$  collisions. The distribution on rapidity  $Y$  of the top quark pair in the final state can be directly computed from Eq. (1), by using its relation with the photon energy  $\omega$ , i.e.,  $Y \propto \ln(\omega/m_t)$ . Explicitly, the rapidity distribution is written down as

$$\begin{aligned} & \frac{d\sigma[h_1 + h_2 \rightarrow h \otimes t\bar{t} + X]}{dY} \\ &= \left[ \omega \frac{dN}{d\omega} \Big|_{h_1} \sigma_{\gamma h_2 \rightarrow t\bar{t}X}(\omega) \right]_{\omega_L} \\ &+ \left[ \omega \frac{dN}{d\omega} \Big|_{h_2} \sigma_{\gamma h_1 \rightarrow t\bar{t}X}(\omega) \right]_{\omega_R}, \end{aligned} \quad (5)$$

where  $\otimes$  represents the presence of a rapidity gap in the final state, and  $\omega_L (\propto e^{-Y})$  and  $\omega_R (\propto e^Y)$  denote photons from the  $h_1$  and  $h_2$  hadrons, respectively. As the photon fluxes, Eqs. (2) and (3), have support at small values of  $\omega$ , decreasing exponentially at large  $\omega$ , the first term on the right-hand side of the Eq. (5) peaks at positive rapidities while the second term peaks at negative rapidities. Consequently, given the photon flux, the study of the rapidity distribution can be used to constrain the photoproduction cross section for a given energy. Moreover, in contrast to the total rapidity distributions for  $pp$  and  $PbPb$  collisions, which will be symmetric about midrapidity ( $Y = 0$ ),  $d\sigma/dY$  will be asymmetric in  $pPb$  collisions due to the differences between the fluxes and process cross sections. Finally, as the maximum value of the photon energy in the flux is determined by the Lorentz factor of the colliding hadrons and the threshold for the top production is very large, the predictions for the top photoproduction cross sections will be strongly dependent on the energy.

In Fig. 2 we present our predictions for  $pp$  and  $PbPb$  collisions at LHC energies. As expected, the total rapidity distributions are symmetric about the midrapidity. In the case of  $pp$  collisions, we calculate  $d\sigma/dY$  considering

different parametrizations for the gluon distribution in the proton. We can see in Fig. 2 (left panel) that the MRST and CT10 predictions are similar, with the MRST one being a lower bound. In Table I we present our estimates for the total cross sections and production rates, assuming the design luminosity  $\mathcal{L}_{\text{LHC}}^{\text{pp}} = 10^7 \text{ mb}^{-1} \text{ s}^{-1}$  and a run time of  $10^7$  seconds. We predict large values for the events rate and cross sections of the order of units of pb, in contrast with values of the order of 160 pb for the inclusive top quark pair hadroproduction [13]. Despite their much smaller cross sections, the clean topology of coherent processes implies a larger signal to background ratio. Therefore, the experimental detection is in principle feasible. However, it is important to emphasize that the signal is expected to be reduced due to the event pileup. An alternative to measure coherent events at the LHC is by tagging the intact hadron in the final state. Such a possibility is currently under study (See, e.g., [24]).

In Fig. 2 (right panel) we present our results for  $PbPb$  collisions. In our calculations we consider that the nuclear gluon distribution is given by  $xg_A = A \cdot R_g \cdot xg_p$ , where  $R_g$  takes into account the nuclear shadowing effects as given by the EPS09 parametrization [23], and  $xg_p$  is the proton-gluon distribution, given by the MRST parameterization [21]. We denote by MRST+EPS09 the predictions obtained including the shadowing effects and by MRST those obtained disregarding these effects, i.e., with  $R_g = 1$ . We can see that the total cross section is reduced by  $\approx 5\%$  by the EMC effect present in the EPS09 parametrization for large values of  $x (\geq 0.4)$ , which implies  $R_g < 1$ . This small contribution of the shadowing effects is expected due to the large value of the hard scale ( $= 4m_t^2$ ) present in the process. Moreover, distinctly from the  $pp$  case,  $d\sigma/dY$  is small at  $Y \approx 0$  and is almost null at  $Y \geq 2$ . It is directly associated to the distinct large- $\omega$  behaviors of the proton and nuclear photon fluxes, with the latter being exponentially suppressed at  $\omega \geq 80 \text{ GeV}$ , while the photon flux of the proton extends up to  $\omega \approx 2400 \text{ GeV}$  (see Table 1 in the last reference of [7]). In Table I we present our estimates

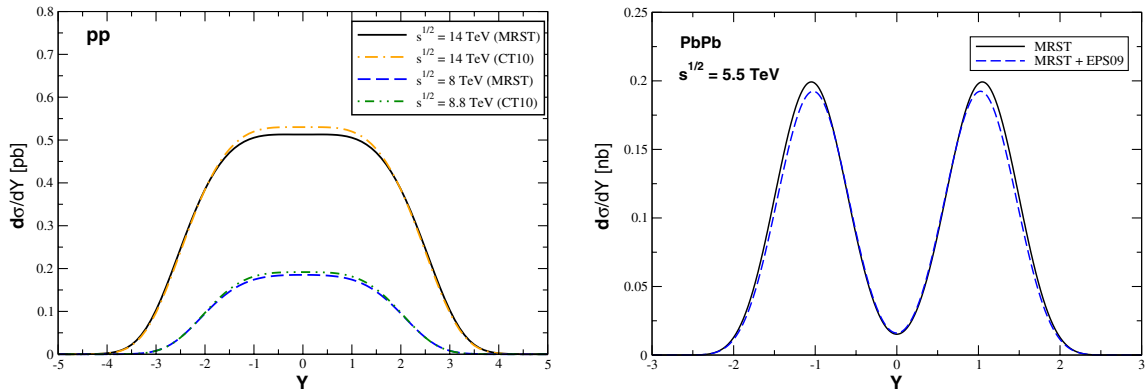


FIG. 2 (color online). Predictions for the rapidity distribution for the photoproduction of top quarks in  $pp$  (left panel) and  $PbPb$  (right panel) collisions at LHC.

TABLE I. The integrated cross section (events rate) for the photoproduction of top quarks in  $pp$ ,  $pPb$ , and  $PbPb$  collisions at LHC energies.

pp	MRST	CT10
$\sqrt{s} = 8$ TeV	0.739 pb (73900)	0.764 pb (76400)
$\sqrt{s} = 14$ TeV	2.50 pb (250000)	2.53 pb (253000)
<hr/>		
pPb	MRST	MRST + EPS09
$\sqrt{s} = 5.5$ TeV	0.036 nb (5.4/3600)	0.038 nb (5.7/3800)
$\sqrt{s} = 8.8$ TeV	0.159 nb (23.85/15900)	0.165 nb (24.75/16500)
<hr/>		
PbPb	MRST	MRST + EPS09
$\sqrt{s} = 5.5$ TeV	0.42 nb (0.18)	0.40 nb (0.17)

for the total cross sections and production rates, assuming the design luminosity  $\mathcal{L}_{\text{LHC}}^{\text{PbPb}} = 0.42 \text{ mb}^{-1} \text{ s}^{-1}$  and a run time of  $10^6$  seconds. Our results indicate that for the default settings and running time, the statistics are marginal for  $PbPb$  collisions.

Let us now discuss the photoproduction of top quarks in  $pPb$  collisions, considering that  $h_1 = Pb$  and  $h_2 = p$ . As discussed before, in this case we expect asymmetric rapidity distributions, with the contribution of the  $\gamma p$  and  $\gamma Pb$  interactions being different. In  $\gamma p$  interactions the photon comes from the nuclei, with the photon flux being proportional to  $Z^2$ , and the photoproduction cross section being determined by the gluon distribution of the proton ( $xg_p$ ). In  $\gamma Pb$  interactions, the photon comes from the proton and the photoproduction cross section being determined by the gluon distribution of the nuclei, which is enhanced by a factor of the order of  $A = 208$  in comparison to  $xg_p$ . As the top quark photoproduction dissociates the target, the experimental separation between the  $\gamma p$  and  $\gamma Pb$  contributions is in principle feasible by analyzing the final state using the zero-degree calorimeters (ZDC) to veto very forward-going neutral fragments and/or by tagging the intact hadron using

forward detectors. In Fig. 3 we explicitly show the different contributions for the rapidity distribution considering two possible values for the  $pPb$  center-of-mass energy and disregarding nuclear shadowing effects. As expected, the  $\gamma Pb$  contribution peaks for negative rapidities and the  $\gamma p$  one for positive rapidities. The rapidity distributions are asymmetric for both energies considered, but the rapidity hemisphere where the maximum of the distribution occurs changes when the energy increases from 5.5 to 8.8 TeV. It is directly associated to the increasing of the  $\gamma p$  contribution with the energy. At  $\sqrt{s} = 5.5$  TeV the  $\gamma Pb$  contribution dominates and the  $\gamma p$  is suppressed due to the large threshold for top production and the small number of high-energy photons in the nuclear photon flux. When  $\sqrt{s}$  increases, a larger number of these photons is present in the flux. Although the  $\gamma Pb$  contribution also is larger for  $\sqrt{s} = 8.8$  TeV, the number of high-energy photons in the nucleus is enhanced by a factor  $Z^2$ , which implies the faster growth of the  $\gamma p$  contribution. Finally, in Fig. 4 we present our predictions considering the nuclear shadowing effects. As in the  $PbPb$  case, the contribution of these effects is small. The basic difference is that in the  $pPb$  case, due to the larger values of  $W_{\gamma h}$  present in the interaction, smaller values of  $x$  are probed. Consequently, the rapidity distribution is enhanced by the antishadowing effects ( $R_g > 1$ ) present in the EPS09 parametrization for  $0.2 \leq x \leq 0.4$ . In Table I we present our estimates for the total cross sections and production rates, assuming the design luminosity  $\mathcal{L}_{\text{LHC}}^{\text{pPb}} = 150 \text{ mb}^{-1} \text{ s}^{-1}$  and a run time of  $10^6$  seconds. We predict cross sections that are a factor of 3 smaller than those obtained in the  $PbPb$  case. The larger  $pA$  luminosity, which is 2 orders of magnitude higher than for  $AA$ , counteracts this suppression for the event rates. However, the resulting event rates still are small. Recently, an upgraded  $pPb$  scenario was proposed in Ref. [25], which improves the  $pPb$  luminosity and the running time. These authors proposed the following scenario for  $pPb$  collisions:  $\mathcal{L}^{\text{pPb}} = 10^4 \text{ mb}^{-1} \text{ s}^{-1}$  and a run

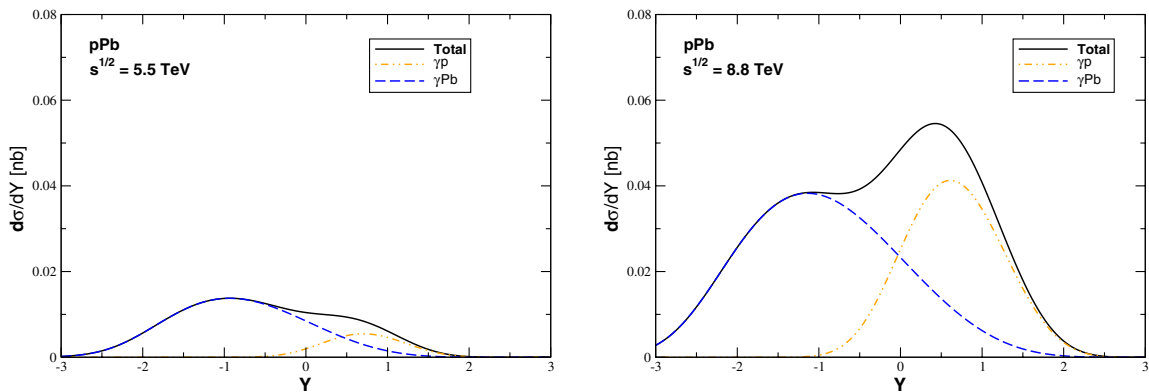


FIG. 3 (color online). Predictions for the rapidity distribution for the photoproduction of top quarks in  $pPb$  collisions at LHC energies:  $\sqrt{s} = 5.5$  TeV (left panel) and  $\sqrt{s} = 8.8$  TeV (right panel). The  $\gamma p$  and  $\gamma Pb$  contributions to the rapidity distributions are presented.

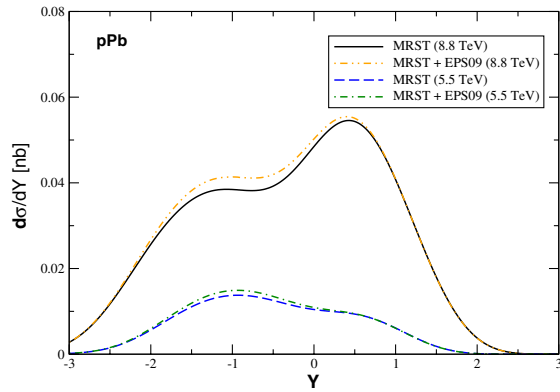


FIG. 4 (color online). Predictions for the rapidity distribution for the photoproduction of top quarks in  $pPb$  collisions at LHC energies considering nuclear shadowing effects.

time of  $10^7$  s. The corresponding event rates also are presented in Table I. In this case we have reasonable numbers, which makes the experimental analysis feasible. Another advantage of  $pPb$  collisions is that they are expected to trigger on and carry out the measurement with almost no pileup [25]. Therefore, the upgraded  $pA$  scenario provides one of the best possibilities to detect the top quark in coherent processes.

Before summarizing our main conclusions, some comments are in order. First, in our calculations the resolved photon contribution was not included. Although it is expected to be small ( $\approx 5\%$ ) for the top quark production, we postpone the study of this subject for a future publication. Second, the top quark can also be produced in single diffractive processes, resulting in a similar topology (one rapidity gap) for the final state, associated to a single

pomeron exchange. Estimates presented in Ref. [26] predict that the cross section for this process in  $pp$  collisions will be of the order of dozens of pb. Although our predictions are smaller than those obtained considering single pomeron interactions, it is expected that emerging hadrons from single diffractive processes have a much larger transverse momentum than those resulting from photoproduction processes. Consequently, in principle it is possible to introduce a selection criteria to separate these two processes. Moreover, it is important to emphasize that the single diffractive predictions are strongly dependent on the value used for the gap survival factor, while our results should not be modified by soft absorption corrections. However, this subject deserves more detailed studies.

As a summary, coherent processes have already been observed at the Tevatron, RHIC, and the LHC with rates in broad agreement with the theoretical predictions. The addition of forward proton taggers at the LHC will enhance the physics potential of the ATLAS, CMS, LHCb, and ALICE detectors to study these processes in more detail. In this paper we present predictions for the photoproduction of top quarks in coherent  $pp/pPb/PbPb$  interactions at the LHC. In particular, we present our predictions for the total cross sections, event rates, and rapidity distributions, and we estimate the magnitude of the nuclear shadowing effects and the dependence of our predictions in the parton distributions. We predict large values for the events rate in  $pp$  collisions and in an upgraded  $pPb$  scenario, which implies that the photoproduction of top quarks should be feasible to study at the CERN LHC.

This work was partially financed by the Brazilian funding agencies CNPq, FAPERGS, and CAPES.

- 
- [1] M. Bedjidian *et al.*, [arXiv:hep-ph/0311048](#).  
[2] V.P. Goncalves and M. V. T. Machado, *Eur. Phys. J. C* **30**, 387 (2003); **32**, 501 (2004); V.P. Goncalves, M. S. Kugeratski, and F. S. Navarra, *Phys. Rev. C* **81**, 065209 (2010).  
[3] D. Boer, M. Diehl, R. Milner, R. Venugopalan, W. Vogelsang, D. Kaplan, H. Montgomery, S. Vignor *et al.*, [arXiv:1108.1713](#).  
[4] J.L. Abelleira Fernandez *et al.* (LHeC Study Group Collaboration), *J. Phys. G* **39**, 075001 (2012).  
[5] V.P. Goncalves and C.A. Bertulani, *Phys. Rev. C* **65**, 054905 (2002); V.P. Goncalves and M. V. T. Machado, *Eur. Phys. J. C* **31**, 371 (2003); *Phys. Rev. D* **71**, 014025 (2005); *Phys. Rev. C* **73**, 044902 (2006); *Phys. Rev. D* **75**, 031502 (2007); V.P. Goncalves, M. V. T. Machado, and A.R. Meneses, *Phys. Rev. D* **80**, 034021 (2009).  
[6] A. Adeluyi and C. Bertulani, *Phys. Rev. C* **84**, 024916 (2011); **85**, 044904 (2012); A. Adeluyi, C.A. Bertulani, and M. J. Murray, *Phys. Rev. C* **86**, 047901 (2012).  
[7] G. Baur, K. Hencken, D. Trautmann, S. Sadovskiy, and Y. Kharlov, *Phys. Rep.* **364**, 359 (2002); C. A. Bertulani, S. R. Klein, and J. Nystrand, *Annu. Rev. Nucl. Part. Sci.* **55**, 271 (2005); A. Baltz, G. Baur, D. Denterria, L. Frankfurt, F. Gelis, V. Guzey, K. Hencken, Y. Kharlov, M. Klasen, and S. Klein, *Phys. Rep.* **458**, 1 (2008).  
[8] T. Aaltonen *et al.* (CDF Collaboration), *Phys. Rev. Lett.* **102**, 242001 (2009).  
[9] C. Adler *et al.* (STAR Collaboration), *Phys. Rev. Lett.* **89**, 272302 (2002).  
[10] S. Afanasiev *et al.* (PHENIX Collaboration), *Phys. Lett. B* **679**, 321 (2009).  
[11] B. Abelev *et al.* (ALICE Collaboration), *Phys. Lett. B* **718**, 1273 (2013).  
[12] Raaij *et al.* (LHCb Collaboration), *J. Phys. G* **40**, 045001 (2013).  
[13] F.-P. Schilling, *Int. J. Mod. Phys. A* **27**, 1230016 (2012).  
[14] S. R. Klein, J. Nystrand, and R. Vogt, *Eur. Phys. J. C* **21**, 563 (2001).

- [15] S. R. Klein and J. Nystrand, *Phys. Rev. C* **60**, 014903 (1999).
- [16] M. Drees and D. Zeppenfeld, *Phys. Rev. D* **39**, 2536 (1989).
- [17] B. A. Kniehl, *Phys. Lett. B* **254**, 267 (1991).
- [18] B. Anderson *et al.* (Small  $x$  Collaboration), *Eur. Phys. J. C* **25**, 77 (2002).
- [19] M. Glück and E. Reya, *Phys. Lett.* **79B**, 453 (1978).
- [20] R. K. Ellis and P. Nason, *Nucl. Phys.* **B312**, 551 (1989); J. Smith and W. L. van Neerven, *Nucl. Phys.* **B374**, 36 (1992).
- [21] A. D. Martin, R. G. Roberts, W. J. Stirling, and R. S. Thorne, *Eur. Phys. J. C* **23**, 73 (2002).
- [22] H.-L. Lai, M. Guzzi, J. Huston, Z. Li, P. M. Nadolsky, J. Pumplin, and C.-P. Yuan, *Phys. Rev. D* **82**, 074024 (2010).
- [23] K. J. Eskola, H. Paukkunen, and C. A. Salgado, *J. High Energy Phys.* 09 (2009) 065.
- [24] ATLAS Collaboration, Report No. CERN-LHCC-2011-0112.
- [25] D. d'Enterria and J. P. Lansberg, *Phys. Rev. D* **81**, 014004 (2010).
- [26] M. V. T. Machado, *Phys. Rev. D* **76**, 054006 (2007).